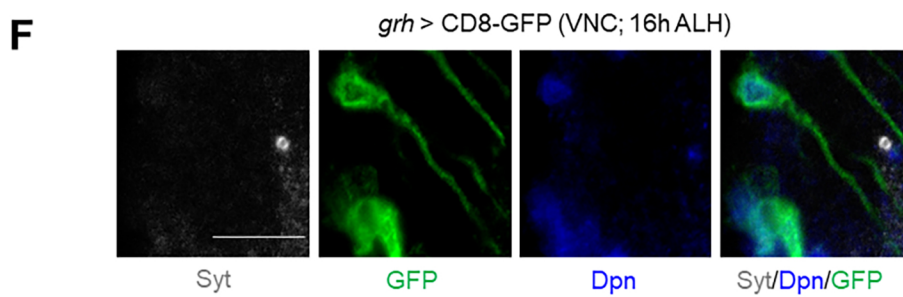
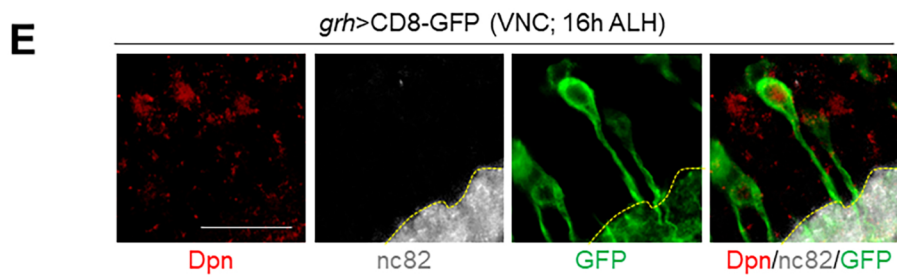
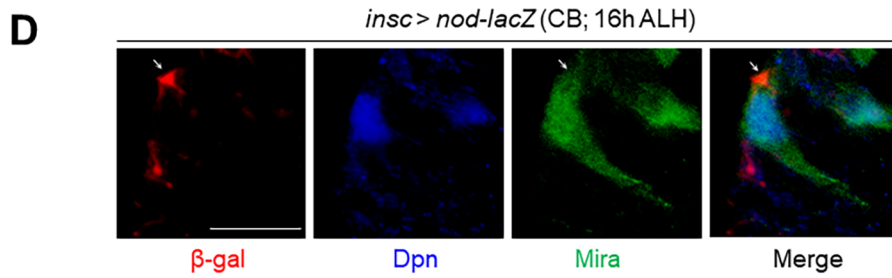
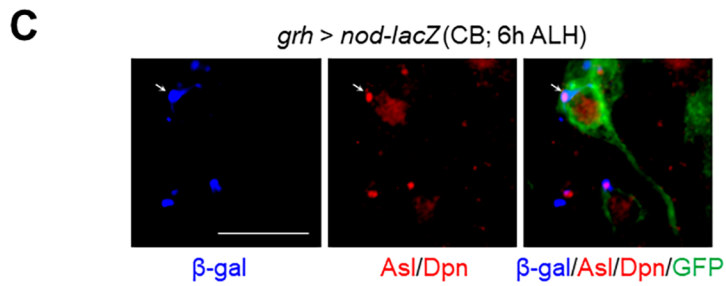
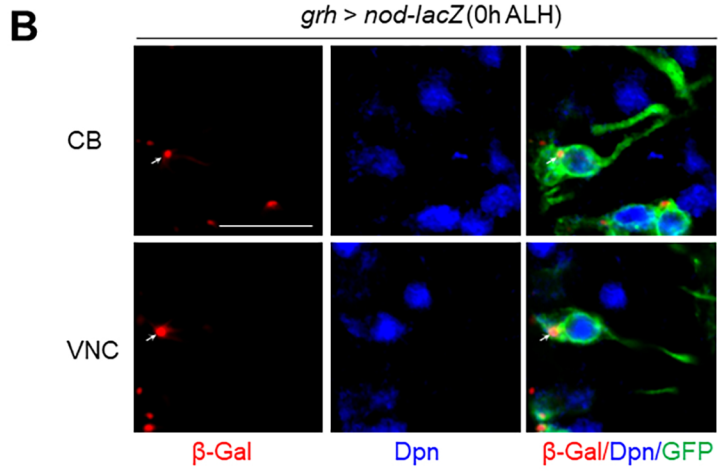
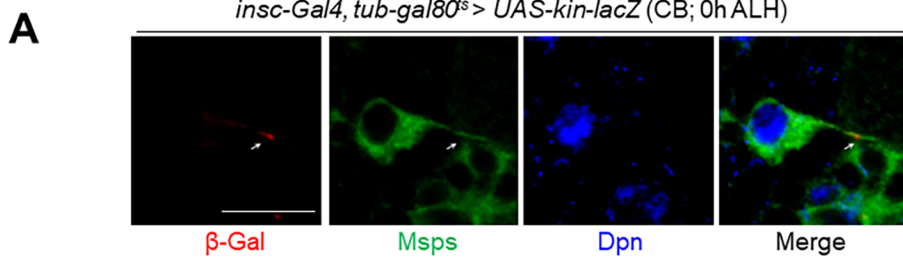


Appendix

Appendix Figure S1. The primary protrusion of qNSCs organizes plus-end-out microtubules.	3
Appendix Figure S2. E-cad is dramatically reduced in NSC-neuropil contact upon <i>E-cad</i> RNAi knockdown in NSCs.	5



Appendix Figure S1. The primary protrusion of qNSCs organizes plus-end-out microtubules.

A) Larval brains at 0 h ALH, in which *kin-lacZ* was expressed under the control of *insc-Gal4*, *tub-Gal80^{ts}*, were labelled with β -Gal, Msps, and Dpn. The primary protrusion of qNSCs was marked by Msps. Quiescent NSCs at the CB are shown.

B) Larval brains at 0 h ALH from *grh-Gal4*; *UAS-nod-lacZ* were labeled with β -gal, Dpn, and GFP. Both the central brain and ventral nerve cord (VNC) are shown.

C) Larval brains at 6 h ALH from *grh-Gal4*; *UAS-nod-lacZ* were labeled with β -gal, Asl, Dpn, and GFP. Quiescent NSCs at the CB are shown.

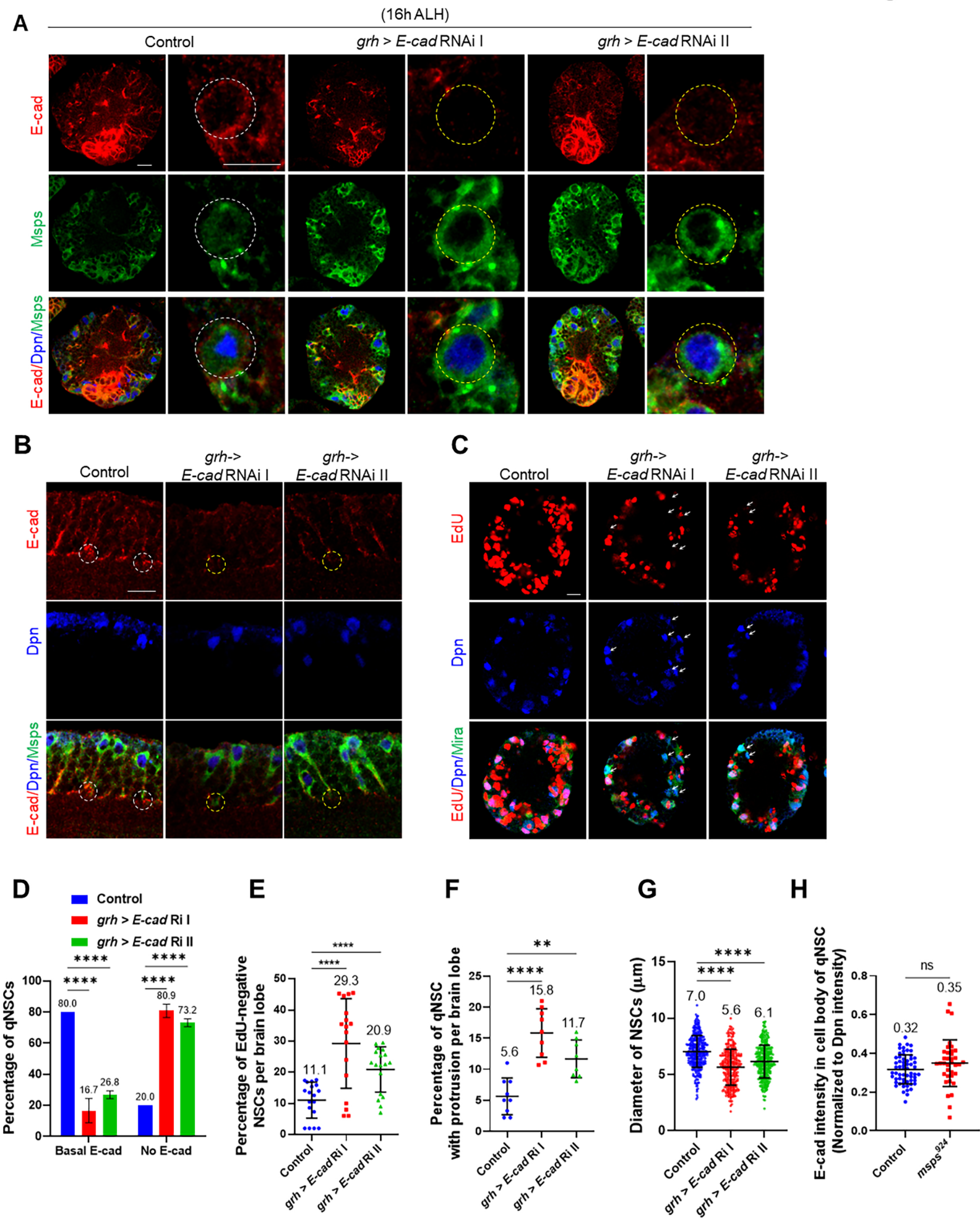
D) Larval brains at 16 h ALH from *insc-Gal4>UAS-nod-lacZ* were labeled with β -gal, Dpn, and Mira. Quiescent NSCs at the CB are shown.

E) Larval brains at 16 h ALH from *grh-Gal4*; *UAS-CD8-GFP* were labeled with nc82, Dpn, and GFP. Nc82 is an antibody that recognizes Bruchpilot at presynaptic sites. Quiescent NSCs at the VNC are shown. Dotted lines indicate the surface of the neuropil.

F) Larval brains at 16 h ALH from *grh-Gal4>UAS-CD8-GFP* were labeled with Synaptotagmin (Syt; A synaptic marker), Dpn, and GFP. Quiescent NSCs at the VNC are shown.

Arrows point at the localization of Kin-lacZ (A) or Nod-lacZ (B-D) in qNSCs.

Scale bars: 10 μ m.



Appendix Figure S2. E-cad is dramatically reduced in NSC-neuropil contact upon *E-cad* RNAi knockdown in NSCs.

A) Larval brains at 16 h ALH from control (*grh-Gal4; UAS-Dicer2/UAS-β-Gal* RNAi), *E-cad* RNAi I, and *E-cad* RNAi II under control of *grh-Gal4; UAS-Dicer2* were labelled with E-cad, Dpn, and Msps. The white dotted lines indicate the outline of NSCs.

B) Larval brains (VNC) at 16 h ALH from control (*grh-Gal4; UAS-Dicer2/UAS-β-Gal* RNAi), *E-cad* RNAi I, and *E-cad* RNAi II under control of *grh-Gal4; UAS-Dicer2* were labeled with E-cad, Dpn, and Msps. Primary protrusion of qNSCs was marked by Msps. The localization of E-cad at the protrusion tip was shown in the dotted circles (control in white; *E-cad* RNAi in yellow).

C) Larval brains at 24 h ALH from control (*grh-Gal4; UAS-dicer2/UAS-β-Gal* RNAi), *E-cad* Ri I (*UAS-E-cad* RNAi (BDSC#32904) and *E-cad* Ri II (*UAS-E-cad* RNAi (BDSC#38207) controlled under *grh-Gal4; UAS-Dicer2* were analyzed for EdU incorporation. EdU-negative NSCs are indicated by arrows.

D) Quantification of E-cadherin basal localization at putative NSC-neuropil contact sites in qNSCs from genotypes in (b). “No E-cad” means absent or strongly reduced E-cad observed at NSC-neuropil contact sites. **** $p < 0.0001$.

E) Quantification graph of EdU-negative NSCs per brain lobe for genotypes in (C). **** $p < 0.0001$.

F) Quantification graph of the percentage of qNSCs with a primary protrusion in control, *E-cad* RNAi I, and *E-cad* RNAi II under *grh-Gal4; UAS-Dicer2*. The protrusion was labelled by Mira. **** $p < 0.0001$; ** $p = 0.0022$.

G) Quantification graph of the diameter of the cell body in NSCs at 24 h ALH from control, *E-cad* RNAi I, and *E-cad* RNAi II under the control of *grh-Gal4; UAS-Dicer2*. NSCs were marked by Dpn and Mira. **** $p < 0.0001$.

Data information: in (D-G), data are presented as mean \pm SD. In (D-G), statistical significances were determined by one-way ANOVA with multiple comparisons. Scale bars: 10 μ m.